EUROGRAPHICS 2003 / P. Brunet and D. Fellner
(Guest Editors)

Volume 22 (2003), Number 3

Compression of 2D Vector Fields Under Guaranteed Topology Preservation

H. Theisel and Ch. Rössl and H.-P. Seidel

MPI Informatik, Saarbrücken, Germany

Abstract

In this paper we introduce a new compression technique for 2D vector fields which preserves the complete topology, i.e., the critical points and the connectivity of the separatrices. As the theoretical foundation of the algorithm, we show in a theorem that for local modifications of a vector field, it is possible to decide entirely by a local analysis whether or not the global topology is preserved. This result is applied in a compression algorithm which is based on a repeated local modification of the vector field - namely a repeated edge collapse of the underlying piecewise linear domain. We apply the compression technique to a number of data sets with a complex topology and obtain significantly improved compression ratios in comparison to pre-existing topology-preserving techniques.

Keywords: *data visualization, flow visualization, vector field compression, vector field topology.*

1. Introduction

Flow visualization is one of the most important subfields of scientific visualization. From its very beginning, flow visualization has had to face the problem of dealing with large and complex data - usually far more complex than a human is able to process, or than computers can transmit and process in acceptable times. Thus most of the flow visualization techniques are somehow involved with compressing and simplifying the flow data, either by visualizing only important parts of the data or by extracting features which contain the most relevant information about the vector field. See [16] for an overview of flow visualization techniques.

One of the most important features of a vector field is its topological skeleton which has been introduced as a visualization tool in [11]. The topological skeleton of a vector field essentially consists of a collection of critical points and special stream lines called separatrices which separate the flow into areas of different flow behavior. The attractiveness of the topological skeleton as a visualization tool lies in the fact that even a complex flow behavior can be expressed (and visualized) by using only a limited number of graphical primitives.

In the original work of [11], only first order critical points were considered, i.e. critical points with a non-vanishing Jacobian. Based on an eigenvector analysis of the Jacobian matrix, these critical points were classified into sources, sinks, centers and saddles. Furthermore, the only separatrices which were considered started from the saddle points in the directions of the eigenvectors of the Jacobian matrix there. In addition, separatrices from detachment and attachment point starting at zero-flow boundaries were considered.

In the following years, this concept of the topological skeleton of a vector field has been extended by considering higher order critical points [17], separatrices starting from boundary switch points [4], closed stream lines [25], critical points at infinity [23], and separation and attachment lines [13]. In [2], the topology of scalar fields is treated for visualization purposes. First approaches for visualizing 3D topological skeletons are in [8].

Flow data sets tend to be large and complex. This fact has motivated intensive research in simplifying and compressing vector fields. For both challenges, topological concepts have been applied. *Topological simplification techniques* apply if the topological complexity of the data set is high and if it is known that certain topological features are due to noise. [4] collapses critical points by using area metrics. [5] proposes two methods: an implicit method (apply a global smoothing over the vector field), and an explicit method (collapse appropriate adjacent first order critical points). In [21], clusters of first order critical points are merged to a higher or-

der critical point. [22] collapses pairs of critical points under preservation of the underlying grid structure of the vector field. [24] analyzes the curvature normal of certain time surfaces to obtain a topology-preserving smoothing of a vector field. The simplification of the topology of scalar fields (which can be considered as a special case of vector field topology) is treated in [6] and [1]. All these topology simplification algorithms mentioned above focus on reducing the number of critical points and do not explicitly treat separatrices. However, since a high number of separatrices starts and ends in critical points, a reduction of the number of critical points also reduces the number of separatrices.

Compression techniques for vector fields are motivated by the necessity of transmitting large flow data sets over networks with low bandwidth, or by the goal to produce visualizations of the data in low-end machines with a small main memory. For these cases the consideration of compressed vector fields makes the process of visual analysis of the flow data more efficient and is sometimes the only way to process the data in reasonable time rates at all. Simple compression techniques ([10], [7], [18]) are based on distance functions which locally compare the vectors of the vector fields without including topological issues. Since the topological skeleton has been proven to describe the vector field in a compact way, it is a natural approach to search for compression techniques which are based on the topology of the vector fields. [15] is a first approach to compress a vector field under the consideration of preserving the characteristics of critical points. Based on a distance measure of vector fields which compares the present critical points, a compression is carried out until the difference of original and compressed vector field exceeds a certain threshold. In [19] a method is introduced which does not only preserve the critical points but also the behavior of the separatrices. This is achieved by extracting the topological skeleton and reconstructing it by a new piecewise linear vector field. For rather simple topologies, this reconstructed piecewise linear vector field turns out to be a compressed version of the original one. However, if the topology of the vector field becomes more complex, the compression ratio drops and might become even negative.

In this paper we introduce a new method of topology preserving vector field compression. Contrary to pre-existing compression methods, our method guarantees that the topology of original and compressed vector field coincides both for critical points and for the connectivity of the separatrices. We show that even under these strong conditions we achieve high compression ratios for vector fields with complex topologies. Our method works on a piecewise linear vector field over a triangulation. We interpret the vector field as a piecewise triangular mesh and adapt a standard mesh reduction algorithm (see e.g. [9]) to this specific problem, i.e. we achieve the compression by iteratively applying half-edge collapses. Before a half-edge collapse is carried out, we have to make sure that it does not change the global topology of the vector field. We show in a theorem that this decision can be made entirely by a local analysis of the vector field in the 1-ring which is affected by a half-edge collapse.

This paper is organized as follows: section 2 gives the theoretical background of vector field topology and shows the theorem on which our compression algorithm is built. This theorem states that – loosely spoken – for local modifications of a vector field it can be decided by a local analysis whether or not the topology is preserved. Section 3 uses this result to introduce our topology-preserving compression algorithm. This algorithm is based on a repeated half-edge collapse of the triangular mesh. Section 4 demonstrates the application of the compression algorithm to flow data sets of a complex topology.

2. Theoretical background

In this section we give the theoretical background of our compression algorithm. The main contribution of this section is to show in theorem 1 that for a local modification of the vector field it can be decided by a local analysis whether the topology is affected by the modification. This property is not evident, since the topology of a vector field is a global feature, and local modifications of the vector field may change the global behavior. To show this property, we have to describe the concept of vector field topology and local modifications in a formal way. Section 2.1 gives a formal description of the topology of a 2D vector field. Section 2.2 discusses the concept of topological equivalence of vector fields. Sections 2.3 treats the impact of local modifications to the topology of a vector field. Section 2.4 discusses further concepts and extensions of the topology of a 2D vector field from the viewpoint of topology preserving local modifications.

2.1. The topology of a 2D vector field

Let $\mathbf{D} \subset \mathbb{E}^2$ be a closed point set which is bounded by n continuous boundary curves $\mathbf{F}_i$ $(i = 0,..,n-1)$. $\mathbf{D}$ serves as the domain of the vector field. Normally, $\mathbf{D}$ is bounded by only one curve, but we particularly allow domains with "holes", i.e. more than one boundary curve. Then a vector field $\mathbf{v}$ is a continuous map $\mathbf{v}: \quad \mathbf{D} \rightarrow \mathbb{R}^2$. We define $\mathbf{C}(\mathbf{v})$ as the set of all critical points of $\mathbf{v}$:

$$\mathbf{C}(\mathbf{v}) = \{\mathbf{x} \in \mathbf{D} \,:\, \mathbf{v}(\mathbf{x}) = (0,0)^T\} \tag{1}$$

and assume that $\mathbf{C}(\mathbf{v})$ is a finite set, i.e., all critical points are isolated. Also, we assume that no critical point lies on one of the boundaries of $\mathbf{D}$. Furthermore, let $\mathbf{v}$ be differentiable in a neighborhood of each critical point, which gives that the Jacobian matrix $\mathbf{J}_\mathbf{v}(\mathbf{x})$ exists for each $\mathbf{x} \in \mathbf{C}(\mathbf{v})$ ([11]). Here we assume that all critical points are first order critical points, i.e. $\det(\mathbf{J}_\mathbf{v}(\mathbf{x})) \neq 0$ holds for all $\mathbf{x} \in \mathbf{C}(\mathbf{v})$. Based on an analysis of $\mathbf{J}_\mathbf{v}$, first order critical points can be classified into saddles, sources, sinks, and centers ([11], [12]). For the description of the topology, saddle points are of particular interest. A saddle $\mathbf{s} \in \mathbf{C}(\mathbf{v})$ is characterized by $\det(\mathbf{J}_\mathbf{v}(\mathbf{s})) < 0$.

Let $\mathbf{F}_i$ be a boundary curve of $\mathbf{D}$. Then $\mathbf{v}$ divides $\mathbf{F}_i$ into a number of consecutive regions of heterogenous outflow and inflow behavior of the vector field [4]. A point $\mathbf{b} \in \mathbf{F}_i$ is called boundary inflow point iff

$$\exists \varepsilon_0 > 0 \ \forall \varepsilon > 0 \ : \ \varepsilon < \varepsilon_0 \Rightarrow (\mathbf{b} + \varepsilon \, \mathbf{v}(\mathbf{b})) \in \mathbf{D}$$

i.e., the flow enters the domain $\mathbf{D}$ there. A point $\mathbf{b} \in \mathbf{F}_i$ is called boundary outflow point iff

$$\exists \varepsilon_0 > 0 \ \forall \varepsilon > 0 \ : \ \varepsilon < \varepsilon_0 \Rightarrow (\mathbf{b} + \varepsilon \, \mathbf{v}(\mathbf{b})) \notin \mathbf{D}$$

i.e., the flow leaves the domain $\mathbf{D}$ there. A point $\mathbf{b} \in \mathbf{F}_i$ is called *boundary switch point* iff in every ε-neighborhood of $\mathbf{b}$ both boundary inflow and outflow points exist. For the case of differentiable boundary curves, boundary switch points are characterized by a flow direction parallel to the tangent direction of the boundary curve in this point. Let $\mathbf{B}(\mathbf{v})$ be the set of all boundary switch points of $\mathbf{v}$.

In the following we assume that $\mathbf{B}(\mathbf{v})$ is a finite set. We consider the boundary switch points on the boundary curve $\mathbf{F}_i$. The points on $\mathbf{F}_i$ which are located between adjacent boundary switch points (while travelling in counterclockwise direction on $\mathbf{F}$) have a similar inflow/outflow behavior: all of them are either boundary inflow points, or all of them are boundary outflow points. We call the set of all points on $\mathbf{F}$ between two adjacent boundary switch points a *boundary inflow region* or *boundary outflow region*. Figure 1a gives an illustration.

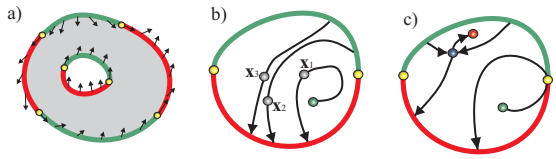

Figure 1: *a) The domain* $\mathbf{D}$ *(gray area) is bounded by two boundary curves. The outer boundary curve has 4 boundary switch points (yellow) which produce two boundary inflow regions (green line) and two boundary outflow regions (red line). The inner boundary curve has 2 boundary switch point producing one boundary inflow region and one boundary outflow region; b) 3 points* $\mathbf{x}_1, \mathbf{x}_2, \mathbf{x}_3$ *and their stream lines;* $\mathbf{x}_2$ *and* $\mathbf{x}_3$ *are stream line equivalent while* $\mathbf{x}_1$ *is not stream line equivalent to* $\mathbf{x}_2$ *or* $\mathbf{x}_3$*; c) topological skeleton of a vector field consisting of 2 boundary switch points (yellow), one boundary outflow region (red line), one boundary inflow region (green line), one saddle point (blue point), one source (green point), one sink (red point), and the separatrices (black lines).*

A *stream line* of $\mathbf{v}$ is a curve in $\mathbf{D}$ with the property that for every point on the curve the tangent direction coincides with the direction of $\mathbf{v}$ in this point ([11]). A particular stream line can be obtained by picking a point $\mathbf{x} \in \mathbf{D}$ and integrating both in forward and backward direction until the stream line either ends in a critical point or leaves $\mathbf{D}$ in a boundary inflow/outflow point (for now we assume that no circulating behavior of a stream line is present). Note that through every non-critical point there is exactly one stream line. Furthermore, stream lines cannot intersect each other (except for critical points). These facts can be used to classify points in $\mathbf{D}$ with respect to the behavior of the stream line through them.

Let $\mathbf{x} \in \mathbf{D}$, and let $\mathbf{S}_\mathbf{v}(\mathbf{x})$ be the stream line through $\mathbf{x}$. $\mathbf{S}_\mathbf{v}(\mathbf{x})$ can be integrated both in forward and backward direction until it ends in a critical point or leaves $\mathbf{D}$ in a boundary inflow/outflow point. We define

Definition 1 Two points $\mathbf{x}_1, \mathbf{x}_2 \in \mathbf{D}$ are *stream line equivalent* concerning $\mathbf{v}$ (written $\mathbf{x}_1 \sim^S_\mathbf{v} \mathbf{x}_2$) if the stream lines through $\mathbf{x}_1$ and $\mathbf{x}_2$ end in the same critical point or inflow/outflow region, for both forward and backward integration.

Figure 1b gives an illustration of definition 1.

The relation $\sim^S_\mathbf{v}$ partitions $\mathbf{D}$ into sectors of similar flow behavior. It is known ([12], [4]) that these sectors are separated by a number of particular stream lines called separatrices. The set of separatrices can be constructed by considering the stream lines from the boundary switch points (both by backward and forward integration), and certain stream lines starting from saddle points.

Every boundary switch point $\mathbf{b}$ is related to two separatrices: one separatrix is obtained by forward integration from $\mathbf{b}$, the other by backward integration. From a saddle point $\mathbf{s}$, four separatrices are constructed: for both eigenvectors of $\mathbf{J}_\mathbf{v}(\mathbf{s})$ in forward and backward direction. This means, we construct separatrices from the four points

$$(\mathbf{s} + \varepsilon \, \mathbf{j}_1) \ , \ (\mathbf{s} - \varepsilon \, \mathbf{j}_1) \ , \ (\mathbf{s} + \varepsilon \, \mathbf{j}_2) \ , \ (\mathbf{s} - \varepsilon \, \mathbf{j}_2)$$

where $\mathbf{j}_1, \mathbf{j}_2$ are the two eigenvectors of $\mathbf{J}_\mathbf{v}(\mathbf{s})$, ε is a very small positive number, and the integration direction is "away from the saddle point". This is justified by the fact that for $\det(\mathbf{J}_\mathbf{v}(\mathbf{s})) \neq 0$, $\mathbf{v}$ is governed by a first order approximation in a neighborhood of $\mathbf{s}$. Using this system of separatrices, each separatrix is uniquely defined by its starting point and its integration direction.

After introducing the concepts above, we can define the topological skeleton of a vector field as the collection of critical points, boundary switch points, and separatrices. Figure 1c illustrates an example.

2.2. Topologically equivalent vector fields

To compare the topology of vector fields, the concept of topological equivalence of two vector fields $\mathbf{v}$ and $\mathbf{w}$ over the same domain $\mathbf{D}$ has to be introduced. Several ways of doing this are possible. One rather restrictive way is to demand that $\mathbf{v}$ and $\mathbf{w}$ coincide in all critical points, their Jacobian matrices, and all separatrices. Since for topologically complex

vector fields the separatrices lie rather densely in the domain, this definition tends to allow only identical vector fields to be equivalent.

On the other hand, a very loose definition of topological equivalence is to demand the coincidence of the structure of the topology graph (i.e., corresponding critical points may vary both in location and in Jacobian, as far as their connectivity of the separatrices coincides.)

Here we want to use a compromise of the above-mentioned definitions:

Definition 2 The vector fields $\mathbf{v}$ and $\mathbf{w}$ over the domain $\mathbf{D}$ are *topologically equivalent* (written $\mathbf{v} \sim_\mathbf{T} \mathbf{w}$) iff the following conditions hold:

i $\mathbf{C}(\mathbf{v}) = \mathbf{C}(\mathbf{w})$
ii $\forall \mathbf{x} \in \mathbf{C}(\mathbf{v}) : \mathbf{J}_\mathbf{v}(\mathbf{x}) = \mathbf{J}_\mathbf{w}(\mathbf{x})$
iii $\mathbf{B}(\mathbf{v}) = \mathbf{B}(\mathbf{w})$
iv Corresponding separatrices in $\mathbf{v}$ and $\mathbf{w}$ end in the same critical point or boundary inflow/outflow region.

Concerning this definition, $\mathbf{v}$ and $\mathbf{w}$ have identical critical points and boundary switch points. Thus $\mathbf{v}$ and $\mathbf{w}$ also have the same number of separatrices. A separatrix in $\mathbf{v}$ corresponds to a separatrix in $\mathbf{w}$ if they start in the same point with the same integration direction.

This definition of topologically equivalent vector fields is rather restrictive to critical points and boundary switch points while giving some freedom to the separatrices. We made this choice because it ensures that topologically equivalent vector fields always have a zero distance concerning all known topology based vector field metrics ([14], [3], [20]).

2.3. Local modifications of the topology

In this section we analyze the effect of local modifications of the vector field and its topology. Since the topology of a vector field is a global feature, local modifications can change the topology everywhere in its domain. Imagine for instance the creation or removal of critical points in the modified area which may affect the separatrices far away from this area.

Nevertheless we show in this section that it can be decided entirely by a local analysis in the area to be modified, whether or not a local modification of the vector field will change its topology.

Let $\mathbf{v}$ and $\mathbf{w}$ be two differentiable vector fields over the domain $\mathbf{D}$, and let $\mathbf{D}' \subset \mathbf{D}$ be a closed subdomain which is bounded by one closed curve $\mathbf{F}'$ (thus assuming that $\mathbf{D}'$ does not have any holes). Furthermore, let $\mathbf{D}'' = (\mathbf{D} \setminus \mathbf{D}') \cup \mathbf{F}'$, and let $\mathbf{v}$ and $\mathbf{w}$ differ only inside $\mathbf{D}'$, i.e.

$$\forall \mathbf{x} \in \mathbf{D}'' : \mathbf{v}(\mathbf{x}) = \mathbf{w}(\mathbf{x}). \tag{2}$$

Figure 2 illustrates an example.

We search for local conditions for $\mathbf{v} \sim_\mathbf{T} \mathbf{w}$. To do so, we collect a number of points on $\mathbf{F}'$. Let $\mathbf{P}_{\mathbf{F}'}(\mathbf{v})$ be the set of all intersection points of all separatrices of $\mathbf{v}$ with $\mathbf{F}'$, and let

$$\mathbf{Q}_{\mathbf{F}'}(\mathbf{v}) = \mathbf{P}_{\mathbf{F}'}(\mathbf{v}) \cup \mathbf{B}(\mathbf{v}|_{\mathbf{D}'})$$

where $\mathbf{v}|_{\mathbf{D}'}$ denotes the vector field $\mathbf{v}$ restricted to the domain $\mathbf{D}'$. Assuming $\mathbf{Q}_{\mathbf{F}'}(\mathbf{v}) \subset \mathbf{F}'$ to be a finite set, we can formulate

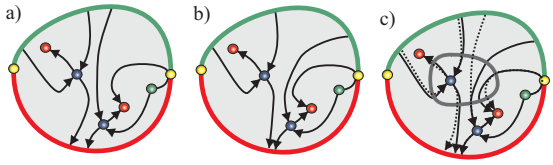

Figure 2: *a) example of a vector field* $\mathbf{v}$ *and its topological skeleton; b) example of a vector field* $\mathbf{w}$ *and its topological skeleton; c) overlay of a) and b):* $\mathbf{v}$ *and* $\mathbf{w}$ *differ only inside the area* $\mathbf{D}'$ *(marked by the inner ring). Stream lines which start in* $\mathbf{D}''$ *coincide in* $\mathbf{v}$ *and* $\mathbf{w}$ *until they enter* $\mathbf{D}'$*. Since they generally leave* $\mathbf{D}'$ *in different points on* $\mathbf{F}'$*, they have different paths in* $\mathbf{D}''$ *after passing through* $\mathbf{D}'$*.*

Theorem 1 The vector fields $\mathbf{v}$ and $\mathbf{w}$ fulfilling (2) are topologically equivalent ($\mathbf{v} \sim_\mathbf{T} \mathbf{w}$) if the following conditions hold:

1. Every separatrix of $\mathbf{v}$ and $\mathbf{w}$ intersects $\mathbf{F}'$ a most once, i.e. has at most one entry point and one exit point with $\mathbf{F}'$.
2. $\mathbf{v}|_{\mathbf{D}'} \sim_\mathbf{T} \mathbf{w}|_{\mathbf{D}'}$.
3. The corresponding points in $\mathbf{Q}_{\mathbf{F}'}(\mathbf{v})$ and $\mathbf{Q}_{\mathbf{F}'}(\mathbf{w})$ are in the same order on $\mathbf{F}'$ (while travelling counterclockwise around $\mathbf{F}'$).

From (2) and condition 2. of theorem 1 it follows that $\mathbf{v}$ and $\mathbf{w}$ have the same critical points and boundary switch points. Hence, the separatrices of $\mathbf{v}$ and $\mathbf{w}$ have a one-to-one correspondence concerning starting point and integration direction. This and condition 1. of theorem 1 gives that there is also a one-to-one correspondence between $\mathbf{P}_{\mathbf{F}'}(\mathbf{v})$ and $\mathbf{P}_{\mathbf{F}'}(\mathbf{w})$: a point $\mathbf{x}_1 \in \mathbf{P}_{\mathbf{F}'}(\mathbf{v})$ corresponds to $\mathbf{x}_2 \in \mathbf{P}_{\mathbf{F}'}(\mathbf{w})$ if their creating separatrices correspond, and both are either entry points or both are exit points of $\mathbf{D}'$ while integrating in integration direction. This unique correspondence between $\mathbf{P}_{\mathbf{F}'}(\mathbf{v})$ and $\mathbf{P}_{\mathbf{F}'}(\mathbf{w})$ (and therefore also between $\mathbf{Q}_{\mathbf{F}'}(\mathbf{v})$ and $\mathbf{Q}_{\mathbf{F}'}(\mathbf{w})$) justifies the formulation of condition 3. of theorem 1.

Theorem 1 means that for checking the topological equivalence of $\mathbf{v}$ and $\mathbf{w}$, we simply have to collect the points of $\mathbf{Q}_{\mathbf{F}'}(\mathbf{v})$ and $\mathbf{Q}_{\mathbf{F}'}(\mathbf{w})$, find the corresponding pairs, and compare their order on $\mathbf{F}'$.

To prove theorem 1 we have to show that the conditions 1.–3. of theorem 1 yield the conditions i–iv of definition 2. Conditions i–iii of definition 2 follow directly from (2) and condition 2. of theorem 1. Only iv of definition 2 remains to be shown. To do so, we construct the topological

skeleton of the vector fields $\mathbf{v}|_{\mathbf{D}''} = \mathbf{w}|_{\mathbf{D}''}$ as shown in figure 3a. This gives $\mathbf{P}_{\mathbf{F}'}(\mathbf{v}|_{\mathbf{D}''}) = \mathbf{P}_{\mathbf{F}'}(\mathbf{w}|_{\mathbf{D}''})$. Furthermore, we

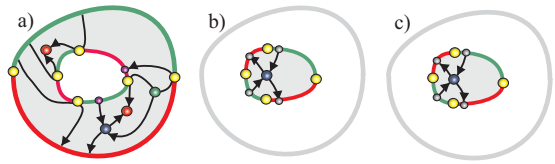

Figure 3: *a) example vector field $\mathbf{v}|_{\mathbf{D}''} = \mathbf{w}|_{\mathbf{D}''}$ (grey area) and its topological skeleton; b) $\mathbf{v}|_{\mathbf{D}'}$ and its topological skeleton: $\mathbf{P}_{\mathbf{F}'}(\mathbf{v}|_{\mathbf{D}'})$ consists of the marked points on the boundary of the grey area; c) $\mathbf{w}|_{\mathbf{D}'}$ and its topological skeleton*

construct the topological skeleton of the vector fields $\mathbf{v}|_{\mathbf{D}'}$ and $\mathbf{w}|_{\mathbf{D}'}$, and compute $\mathbf{P}_{\mathbf{F}'}(\mathbf{v}|_{\mathbf{D}'})$ and $\mathbf{P}_{\mathbf{F}'}(\mathbf{w}|_{\mathbf{D}'})$. Figures 3b and 3c illustrate this. Condition 2. of theorem 1 ensures that there is a one-to-one correspondence between $\mathbf{P}_{\mathbf{F}'}(\mathbf{v}|_{\mathbf{D}'})$ and $\mathbf{P}_{\mathbf{F}'}(\mathbf{w}|_{\mathbf{D}'})$. Also, we have

$$\mathbf{P}_{\mathbf{F}'}(\mathbf{v}|_{\mathbf{D}''}) \cup \mathbf{P}_{\mathbf{F}'}(\mathbf{v}|_{\mathbf{D}'}) \subseteq \mathbf{Q}_{\mathbf{F}'}(\mathbf{v}),$$
$$\mathbf{P}_{\mathbf{F}'}(\mathbf{w}|_{\mathbf{D}''}) \cup \mathbf{P}_{\mathbf{F}'}(\mathbf{w}|_{\mathbf{D}'}) \subseteq \mathbf{Q}_{\mathbf{F}'}(\mathbf{w}).$$

This and condition 3. of theorem 1 ensure that corresponding points of $\mathbf{P}_{\mathbf{F}'}(\mathbf{v}|_{\mathbf{D}''}) \cup \mathbf{P}_{\mathbf{F}'}(\mathbf{v}|_{\mathbf{D}'})$ and $\mathbf{P}_{\mathbf{F}'}(\mathbf{w}|_{\mathbf{D}''}) \cup \mathbf{P}_{\mathbf{F}'}(\mathbf{w}|_{\mathbf{D}'})$ are in the same order on $\mathbf{F}'$.

The joint of the topological skeletons of $\mathbf{v}|_{\mathbf{D}'}$ and $\mathbf{v}|_{\mathbf{D}''}$ does not yield the topological skeleton of $\mathbf{v}$ yet. In fact, all separatrices which intersect $\mathbf{F}'$ end there. Figure 4 illustrates this. To complete the topological skeleton of $\mathbf{v}$, we have to

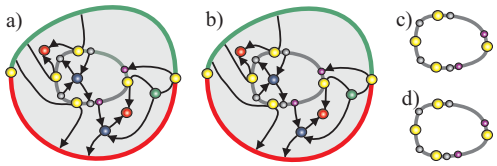

Figure 4: *a) joining the topological skeletons of $\mathbf{v}|_{\mathbf{D}'}$ and $\mathbf{v}|_{\mathbf{D}''}$ does not yield the topological skeleton of $\mathbf{v}$, since the separatrices of $\mathbf{v}|_{\mathbf{D}'}$ and $\mathbf{v}|_{\mathbf{D}''}$ end when crossing $\mathbf{F}'$; b) joining the topology of $\mathbf{w}|_{\mathbf{D}'}$ and $\mathbf{w}|_{\mathbf{D}''}$; c) $\mathbf{P}_{\mathbf{F}'}(\mathbf{v}|_{\mathbf{D}''}) \cup \mathbf{P}_{\mathbf{F}'}(\mathbf{v}|_{\mathbf{D}'})$ consists of the marked points on $\mathbf{F}'$; d) $\mathbf{P}_{\mathbf{F}'}(\mathbf{w}|_{\mathbf{D}''}) \cup \mathbf{P}_{\mathbf{F}'}(\mathbf{w}|_{\mathbf{D}'})$*

do the following constructions:

A continue the integration of all separatrices of $\mathbf{v}|_{\mathbf{D}'}$ if they leave $\mathbf{D}'$ in a point on $\mathbf{F}'$,

B continue the integration of all separatrices of $\mathbf{v}|_{\mathbf{D}''}$ if they leave $\mathbf{D}''$ in a point on $\mathbf{F}'$.

(The similar statement holds for the vector field $\mathbf{w}$.) Concerning A mentioned above, let $\mathbf{S}_1$ be a separatrix in $\mathbf{v}|_{\mathbf{D}'}$, and let $\mathbf{S}_2$ be the corresponding separatrix in $\mathbf{w}|_{\mathbf{D}'}$. This means that $\mathbf{S}_1$ and $\mathbf{S}_2$ start from the same point in the same integration direction. Let $\mathbf{S}_1$ intersect $\mathbf{F}'$ in the point $\mathbf{x}_1$, and let $\mathbf{S}_2$ intersect $\mathbf{F}'$ in $\mathbf{x}_2$. In general, $\mathbf{x}_1$ and $\mathbf{x}_2$ differ. Nevertheless, from condition 3. of theorem 1 we know that $\mathbf{x}_1$ and $\mathbf{x}_2$ are located between the same adjacent points of $\mathbf{P}_{\mathbf{F}'}(\mathbf{v}|_{\mathbf{D}''}) = \mathbf{P}_{\mathbf{F}'}(\mathbf{w}|_{\mathbf{D}''})$. This means that $\mathbf{x}_1$ and $\mathbf{x}_2$ are not separated by a separatrix in $\mathbf{v}|_{\mathbf{D}''} = \mathbf{w}|_{\mathbf{D}''}$. Hence the integration of the stream lines in $\mathbf{D}''$ starting from $\mathbf{x}_1$ and $\mathbf{x}_2$ ends in the same critical point or boundary inflow/outflow region: the separatrices $\mathbf{S}_1$ and $\mathbf{S}_2$ in the whole domain $\mathbf{D}$ are corresponding.

Concerning B mentioned above, let $\mathbf{S}_1$ be a stream line in $\mathbf{v}|_{\mathbf{D}''}$, let $\mathbf{S}_2 = \mathbf{S}_1$ be the corresponding stream line in $\mathbf{w}|_{\mathbf{D}''}$, and let $\mathbf{x} \in \mathbf{P}_{\mathbf{F}'}(\mathbf{v}|_{\mathbf{D}'})$ be the intersection of $\mathbf{S}_1$ and $\mathbf{S}_2$ with $\mathbf{F}'$. We integrate $\mathbf{S}_1$ in $\mathbf{D}'$ from $\mathbf{x}$ until $\mathbf{S}_1$ leaves $\mathbf{D}'$ in a point $\mathbf{x}_1 \in \mathbf{F}'$. Also, we integrate $\mathbf{S}_2$ in $\mathbf{D}'$ from $\mathbf{x}$ until $\mathbf{S}_2$ leaves $\mathbf{D}'$ in a point $\mathbf{x}_2 \in \mathbf{F}'$. Figure 5 illustrates this. Since

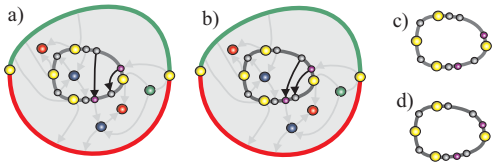

Figure 5: *a) continue integrating separatrices of $\mathbf{v}|_{\mathbf{D}''}$ if they enter $\mathbf{D}'$; b) continue integrating separatrices of $\mathbf{w}|_{\mathbf{D}''}$ if they enter $\mathbf{D}'$; c) $\mathbf{Q}_{\mathbf{F}'}(\mathbf{v})$ consists of the marked points; d) $\mathbf{Q}_{\mathbf{F}'}(\mathbf{w})$ consists of the marked points.*

$\mathbf{x}_1 \in \mathbf{Q}_{\mathbf{F}'}(\mathbf{v})$, $\mathbf{x}_2 \in \mathbf{Q}_{\mathbf{F}'}(\mathbf{w})$, and condition 3. of theorem 1, $\mathbf{x}_1$ and $\mathbf{x}_2$ are located between the same adjacent points of $\mathbf{P}_{\mathbf{F}'}(\mathbf{v}|_{\mathbf{D}''}) = \mathbf{P}_{\mathbf{F}'}(\mathbf{w}|_{\mathbf{D}''})$ on $\mathbf{F}'$. Then the same argumentation as in A gives that $\mathbf{S}_1$ and $\mathbf{S}_2$ are corresponding in the whole domain $\mathbf{D}$, which proves theorem 1.

2.4. Extensions of the topology concept

In section 2.1 we made a number of simplifying assumptions about the considered vector fields in order to keep the proof of theorem 1 simple. Although many practical vector fields (including our examples in the next section) fulfill these assumptions, there are vector fields with different topological structures. In this section we discuss the applicability of theorem 1 to these vector fields:

- Zero flow boundaries:
  Zero flow boundaries are present if for instance the flow around certain solids is simulated. Instead of boundary switch points, attachment and detachment points divide the boundary curve there. The proof of theorem 1 was only based on the fact that the topological skeleton provides a complete partition to areas of similar flow behavior. If this condition is fulfilled by the additional consideration of attachment and detachment points, theorem 1 can also be applied for vector fields with zero-flow boundaries.

- Closed separatrices:
  Vector fields may have additional closed stream lines as separatrices. These separatrices do not have a unique starting point. Moreover, condition 1. of theorem 1 is not fulfilled if such a separatrix intersects $\mathbf{D}'$. Hence the conditions of theorem 1 are not fulfilled if closed separatrices enter $\mathbf{D}'$.
- Higher order critical points:
  If higher order critical points are present, the regions of similar flow behavior around them are separated by a number of separatrices. Since these separatrices have a unique starting point, theorem 1 can be applied.

3. Compressing the vector field

In this section we apply the results of section 2 to build an algorithm for topology preserving compression of 2D vector fields. The algorithm works on a piecewise linear original vector field. This means, given is a triangulation of the domain with velocity information in every vertex. This way the vector field can be considered as a triangular mesh; the problem of compressing the vector data set is thus converted to a mesh reduction problem.

Techniques for solving this simplification problem have been studied extensively during the last decade, see e.g. [9] for a recent and comprehensive survey. We choose the so called *half-edge collapse* as basic removal operator. It collapses a vertex $\mathbf{p}_0$ into its neighbor $\mathbf{p}_1$ along the directed edge $(\mathbf{p}_0, \mathbf{p}_1)$ (see figures 7c and 7d for an example). Before a half-edge collapse is applied, we have to make sure that it does not change the topology of the vector field. We describe the algorithm for doing so in section 3.2. Section 3.1 describes the necessary data structures for the algorithm. Section 3.3 describes the whole compression algorithm.

3.1. The data structure

As a preprocess of the algorithm, we have to extract the topology of the original piecewise linear vector field and store it in an appropriate data structure. This data structure is essentially a triangular mesh with vector information at each vertex. In addition, each triangle has information about present critical points, boundary switch points and separatrices. If a critical point appears inside the triangle, its location and classification is stored with the triangle. If there is a boundary switch point in a boundary triangle, its location is stored with the triangle. Starting from the boundary switch points and saddle points, the separatrices are integrated over the vector field. This way a separatrix usually passes through a number of triangles. For each of these triangles the following items are stored:

- ID of the separatrix
- entry point into triangle (or starting point of the integration if the separatrix origins inside the triangle) in integration direction
- exit point out of triangle (or critical point inside the triangle where the separatrix ends) in integration direction

Note that the integration direction is not necessarily the flow direction of the vector field. Instead, the integration direction is always "away from" its originating saddle point or boundary switch point.

3.2. Controlled half-edge collapse

Based on the mesh data structure described above, we can apply the results of theorem 1 to locally check whether a half-edge collapse changes the topology of the vector field. Let $\mathbf{p}_0, \mathbf{p}_1$ be two vertices which are connected by an edge, let $\mathbf{p}_1, ..., \mathbf{p}_n$ be the 1-ring around $\mathbf{p}_0$, and let $\mathbf{t}_1, ..., \mathbf{t}_n$ be the (counterclockwise ordered) triangles around $\mathbf{p}_0$. Figure 6a illustrates this. A half-edge collapse $\mathbf{p}_0 \rightarrow \mathbf{p}_1$ only affects

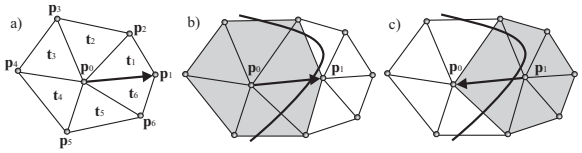

Figure 6: *a) a half-edge collapse $\mathbf{p}_0 \rightarrow \mathbf{p}_1$ only affects the vector field inside the triangles $\mathbf{t}_1, ..., \mathbf{t}_n$; b) example of an impossible half-edge collapse $\mathbf{p}_0 \rightarrow \mathbf{p}_1$ because one separatrix enters $\mathbf{D}'$ (marked grey) twice; c) for the same configuration as b), the half-edge collapse $\mathbf{p}_1 \rightarrow \mathbf{p}_0$ may be allowed because the separatrix enters $\mathbf{D}'$ (marked grey) only once.*

the vector field inside the triangles $\mathbf{t}_1, ..., \mathbf{t}_n$. This is the area $\mathbf{D}'$ of theorem 1 in which local modifications of the vector field take place.

Now we can describe the algorithm to check whether a half-edge collapse changes the topology of a vector field:

Algorithm 1

1 Check if there are critical points inside $\mathbf{D}' = (\mathbf{t}_1, ..., \mathbf{t}_n)$. If so, stop and prohibit the half-edge collapse.
2 Collect all separatrices which pass through $\mathbf{D}'$. For each separatrix, store entry point and exit point of $\mathbf{D}'$ in a cyclic list L_1 which is ordered concerning the order of the points on the closed polygon $((\mathbf{p}_1, \mathbf{p}_2), ..., (\mathbf{p}_{n-1}, \mathbf{p}_n), (\mathbf{p}_n, \mathbf{p}_1))$.
3 If a separatrix enters $\mathbf{D}'$ more than once, stop and prohibit the half-edge collapse.
4 Compute the boundary switch points of the vector field on the polygon $((\mathbf{p}_1, \mathbf{p}_2), ..., (\mathbf{p}_{n-1}, \mathbf{p}_n), (\mathbf{p}_n, \mathbf{p}_1))$, insert these points to L_1.
5 Simulate the half-edge collapse $\mathbf{p}_0 \rightarrow \mathbf{p}_1$ while storing the original configuration (to allow an undo of the half-edge collapse).
6 Apply linear interpolation of the vector field inside the new triangles $(\mathbf{p}_1, \mathbf{p}_2, \mathbf{p}_3), (\mathbf{p}_1, \mathbf{p}_3, \mathbf{p}_4), ..., (\mathbf{p}_1, \mathbf{p}_{n-1}, \mathbf{p}_n))$. Check

whether there are critical points inside one of the new triangles. If so, stop and prohibit half-edge collapse.

7 Construct a new cyclic ordered list L_2 of points on the polygon $((\mathbf{p}_1,\mathbf{p}_2),...,(\mathbf{p}_{n-1},\mathbf{p}_n),(\mathbf{p}_n,\mathbf{p}_1))$ consisting of the following points:

   a. all boundary switch points of step 4 of the algorithm
   b. the entry points of all separatrices to $\mathbf{D}'$
   c. integrate the stream lines starting from all points of step 7b. of this algorithm inside $\mathbf{D}'$ until they reach the boundary again; store the exit points in L_2.

8 Undo simulated half-edge collapse $\mathbf{p}_0 \rightarrow \mathbf{p}_1$

9 Compare the cyclic order of the points in L_1 and L_2. If the corresponding points do not have the same cyclic order in $L_1$and L_2, stop and prohibit the half-edge collapse.

10 Stop and allow the half-edge collapse.

Figure 7 illustrates this algorithm where an edge collapse is allowed. Figure 8 shows an example where the algorithm prohibits an edge collapse.

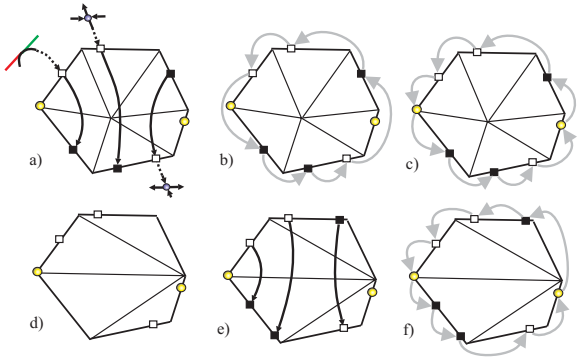

Figure 7: *Example of algorithms 1; a) 3 separatrices passing through* $\mathbf{D}'$*, and 2 boundary switch points (yellow) are present; the empty boxes are the entry points of the separatrices into* $\mathbf{D}'$ *(in integration direction), the solid boxes describe the exit points; b) cyclic list* L_1 *(grey arrows) after step 2; c)* L_1 *after step 4; d) collecting points of new list* L_2 *after half-edge collapse: after step 7a. and 7b.; e) integrate new stream lines (7c.); f) cyclic list* L_2 *after step 7c.; edge collapse is allowed, since the corresponding points in* L_1 *and* L_2 *(shown in c) and f)) are in same order.*

Algorithm 1 needs some remarks:

- The collected points in the lists L_1 and L_2 correspond to $\mathbf{Q}_{\mathbf{F}'}(\mathbf{v})$ and $\mathbf{Q}_{\mathbf{F}'}(\mathbf{w})$ of theorem 1. Moreover, steps 1 and 6 of algorithm 1 ensure condition 2. of theorem 1, and step 2 ensures condition 1. of theorem 1. Hence theorem 1 proves the correctness of algorithm 1.
- The entire algorithm works locally on the 1-ring around $\mathbf{p}_0$.
- If an edge collapse is impossible because of a re-entry of a separatrix, an edge collapse of an adjacent edge (or of the opposite half-edge) might still be possible. Figures 6b and 6c show an example.

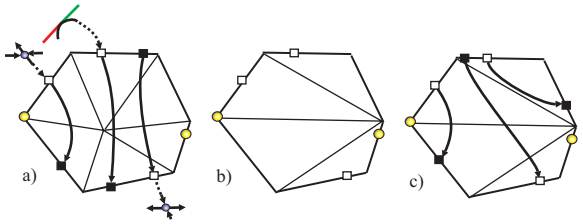

Figure 8: *a) Another example of algorithms 1; a) 3 separatrices passing through* $\mathbf{D}'$*, and 2 boundary switch points (yellow) are present:* L_1 *consists of the marked points on the boundary; b) points of* L_2 *after step 7b.; c) points of* L_2 *after step 7c.; edge collapse is not allowed, since the corresponding points in* L_1 *and* L_2 *(shown in a) and c)) are in different order.*

3.3. The compression algorithm

The vector field compression is achieved by applying a mesh reduction to the triangulated domain of the piecewise linear vector field. A standard algorithm is adapted to this specific problem. Its basic topological operator is the *controlled* half-edge collapse from section 3.2. The mesh reduction algorithm can now be sketched as follows:

Algorithm 2
Repeat...

1 *Initialization.* For all directed edges $(\mathbf{p}_i,\mathbf{p}_j)$:

   a. Apply *Algorithm 1* to check whether half-edge collapse is allowed.
   b. If allowed: evaluate priority and put $(\mathbf{p}_0,\mathbf{p}_1)$ into priority queue **PQ**

2 *Iterative removal.* **While PQ** not empty

   a. Get and remove $(\mathbf{p}_i,\mathbf{p}_j)$ from **PQ**.
   b. If half-edge collapse $(\mathbf{p}_i,\mathbf{p}_j)$ allowed: apply half-edge collapse $(\mathbf{p}_i,\mathbf{p}_j)$.
   c. Update topology data structure.
   d. Reapply **Algorithm 1** to all edges incident to $\mathbf{p}_j$ and to $\mathbf{p}_j$'s 1-ring, and update **PQ** accordingly.

...**until** no more collapses possible.

Here, the inner loop reflects the standard mesh reduction algorithm. The outer loop that causes repeated reinitialization reflects the fact that local changes may have global impact and may thus allow collapses that have been prohibited before. The update o the topology data structure (step 2c.) of algorithm 2) is the most expensive part of the algorithm. If a half-edge collapse is carried out, the topology data structure (described in section 3.1 has to be updated: all separatrices

which pass through the 1-ring around $\mathbf{p}_0$ have to be reintegrated from their entrance point into the 1-ring.

The whole process is a greedy optimization driven by a priority queue. In a 3D setup the priority of a collapse would be some kind of quality measure as e.g. distance to the original surface. In the 2D case we are left with an additional degree of freedom. A natural choice would be to locally apply some difference measure for flow fields ([7], [10]). In our current implementation we merely assign priorities proportional to edge lengths, preferring short edges for collapse.

4. Results

We applied our compression algorithm to two test data sets. The first data set describes (the perpendicular of) the flow of a bay area of the Baltic Sea near Greifswald (Germany). The data set was created by the Department of Mathematics, University of Rostock (Germany). The data was given as an incomplete flow data set on a regular 115 x 103 grid. Applying a triangulation of the defined cells, we have a piecewise linear vector field consisting of 14,086 triangles (see figure 9a). Figure 9e shows the topological skeleton of the vector field while figure 9c shows its LIC image. This flow data set consists of 71 critical points, 44 boundary switch points, and 168 separatrices. Applying our compression algorithm, we obtained a new piecewise linear vector field which consists of 660 triangles. Figure 9b shows the piecewise triangular domain of the compressed vector field. Figure 9d shows the LIC image, and figure 9f shows the topological skeleton of the compressed vector field. Note that the topological skeletons of original and compressed vector field (figures 9e and 9f) are equivalent concerning definition 2. The compression ratio is 95.3%. The complete compression algorithm took 280 seconds on an Intel Xeon 1.7 GHz processor.

The second test data set describes the skin friction on a face of a cylinder which was obtained by a numerical simulation of a flow around a square cylinder. The data set was generated by R.W.C.P. Verstappen and A.E.P. Veldman of the University of Groningen (the Netherlands). The same data set has been analyzed in [4] and [15]. The data was given on a rectangular 102 x 64 grid with varying grid size. To get a piecewise linear vector field, we divided each grid cell in two triangles which gives a piecewise triangular domain consisting of 12,726 triangles. Figure 10a shows the piecewise triangular domain of the vector field. As we can see in this picture, all triangles there tend to be large and thin. Figure 10c shows the LIC image of the vector field while figure 10e shows its topological skeleton. This vector field consists of 338 critical points, 34 boundary switch points, and 714 separatrices. Therefore, it can be considered as a vector field of a complex topology. After applying our compression algorithm, we obtained a vector field with the piecewise triangular domain shown in figure 10b. This domain consists of 2,153 triangles which gives a compression ratio of 83.1 %. Figure 10d shows the LIC image of the compressed vector field, figure 10f shows the topological skeleton. The complete compression algorithm took 299 seconds on an Intel Xeon 1.7 GHz processor.

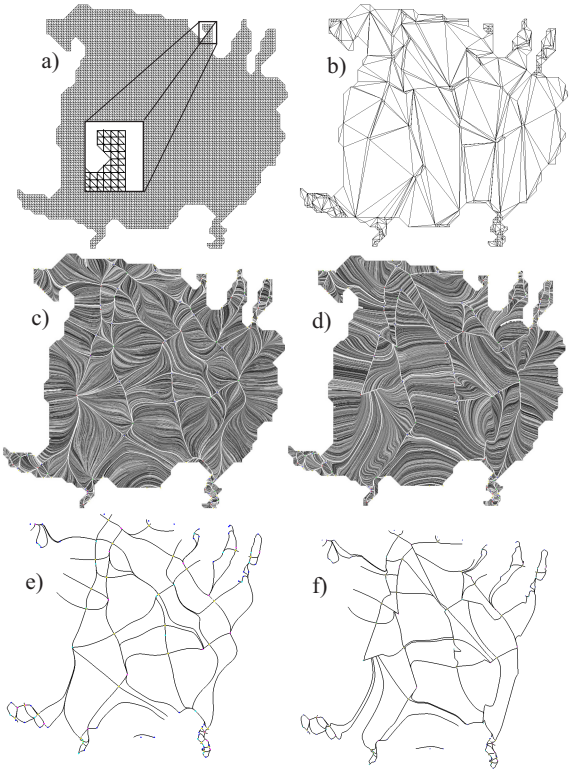

Figure 9: *Test data set 1 (flow in a bay area near Greifswald); a) piecewise triangular domain of the original data set; b) piecewise triangular domain of the compressed data set; c) LIC of original data set; d) LIC of compressed data set; e) topological skeleton of original data set; f) topological skeleton of compressed data set.*

Because of the high complexity of the data set, the visualizations in figure 10 appear to be cluttered. Therefore, we present two magnifications of the skin friction data set in figures 11 and 12. The larger rectangle in figure 10c denotes the magnified area considered in figure 11; the smaller rectangle rectangle of figure 10c is magnified in figure 12. Note that the topological skeletons of the original (figure 10e) and the compressed vector field (figure 10f) are equivalent, even though separatrices in the compressed flow tend to be very close together.

5. Conclusions and Future research

We have introduced a new compression technique for 2D vector fields which preserves the topological skeleton of the vector field. Our examples have shown that even for

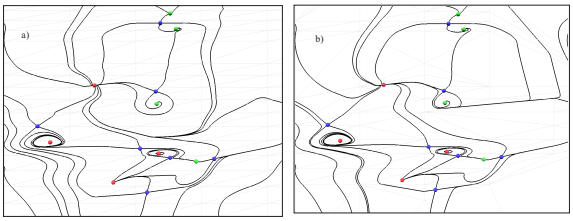

Figure 12: *Magnification of test data set 2; a) topological skeleton and underlying grid of original data set; b) topological skeleton and underlying grid of compressed data set;*

topologically complex data sets high compression ratios are achieved. Now we compare these compression ratios with pre-existing topology preserving compression techniques.

[15] analyzed the same skin friction data set as we do, but uses a significantly less strict definition of topology. In fact, small changes of the Jacobian of critical points are permitted, and separatrices are not considered at all. Even with this less strict topology concept, the compression ratio under topology preservation (37 %) is significantly less than ours. [19] uses a topology concept similar to the one used here, i.e., [19] considers the complete Jacobian matrix of the critical points as well as the connectivity of the separatrices. The compression algorithm presented there can only be applied for data sets with a rather simple topology. For vector fields with a topological complexity as in our examples, very low or even negative compression ratios have to be expected.

We conclude that our new algorithm gives significantly better compression ratios than known existing topology-preserving compression techniques when applied to topologically complex data sets.

For future research, we see the following open questions:

- Up to now, research on vector field topology had focused either on the topological simplification or a topology preserving compression. Combinations of both techniques seem to be an interesting task. The main problem there is to decide which parts of the topology are relevant, and which parts can be removed by simplification before topology preserving compression techniques are applied.
- We considered our vector fields to be a flat triangular mesh with velocity information in each vertex. The same approach can also be applied to vector fields on (general) triangular meshes. Here the interplay between vector field compression techniques and mesh modification techniques can be studied.

Acknowledgements

The authors thank Wim de Leeuw for providing the skin friction data set.

References

1. C. Bajaj and D. Schikore. Topology-preseving data simplification with error bounds. *Comput. & Graphics*, 22(1):3–12, 1998. 2
2. C.L. Bajaj, V. Pascucci, and D.R. Schikore. Visualization of scalar topology for structural enhancement. In *Proc. IEEE Visualization '98*, pages 51–58, 1998. 1
3. R. Batra, K. Kling, and L. Hesselink. Topology based vector field comparison using graph methods. In *Proc. IEEE Visualization '98, Late Breaking Hot Topics*, pages 25–28, 1998. 4
4. W. de Leeuw and R. van Liere. Collapsing flow topology using area metrics. In *Proc. IEEE Visualization '99*, pages 149–354, 1999. 1, 3, 8
5. W.C. de Leeuw and R. van Liere. Visualization of global flow structures using multiple levels of topology. In *Proc. VisSym 99*, pages 45–52, 1999. 1
6. H. Edelsbrunner, J. Harer, and A. Zomorodian. Hierarchical morse complexes for piecewise linear 2-manifolds. In *Proc. 17th Sympos. Comput. Geom. 2001*, 2001. 2
7. H. Garcke, T. Preusser, M. Rumpf, A. Telea, U. Weikardt, and J. van Wijk. A continuous clustering method for vector fields. In *Proc. IEEE Visualization 2000*, pages 351–358, 2000. 2, 8
8. A. Globus and C. Levit. A tool for visualizing of three-dimensional vector fields. In *Proc. IEEE Visualization '91*, pages 33–40, 1991. 1
9. C. Gotsman, S. Gumhold, and L. Kobbelt. Simplification and compression of 3D meshes. In A. Iske, E. Quak, and M. S. Floater, editors, *Tutorials on Multiresolution in Geometric Modelling*, Mathematics and Visualization, pages 319–361. Springer, 2002. 2, 6
10. B. Heckel, G.H. Weber, B. Hamann, and K.I.Joy. Construction of vector field hierarchies. In *Proc. IEEE Visualization '99*, pages 19–26, 1999. 2, 8
11. J. Helman and L. Hesselink. Representation and display of vector field topology in fluid flow data sets. *IEEE Computer*, 22(8):27–36, August 1989. 1, 2, 3
12. J. Helman and L. Hesselink. Visualizing vector field topology in fluid flows. *IEEE Computer Graphics and Applications*, 11:36–46, May 1991. 2, 3
13. D.N. Kenwright, C. Henze, and C. Levit. Feature extraction of separation and attachment lines. *IEEE Transactions on Visualization and Computer Graphics*, 5(2):135–144, 1999. 1
14. Y. Lavin, R.K. Batra, and L. Hesselink. Feature comparisons of vector fields using earth mover's distance. In *Proc. IEEE Visualization '98*, pages 103–109, 1998. 4
15. S.K. Lodha, J.C. Renteria, and K.M. Roskin. Topology preserving compression of 2D vector fields. In *Proc. IEEE Visualization 2000*, pages 343–350, 2000. 2, 8, 9
16. F.H. Post, B. Vrolijk, H. Hauser, R.S. Laramee, and H. Doleisch. Feature extraction and visualisation of flow fields. In *Proc. Eurographics 2002, State of the Art Reports*, pages 69–100, 2002. 1
17. G. Scheuermann, H. Krüger, M. Menzel, and A. Rockwood. Visualizing non-linear vector field topology. *IEEE Transactions on Visualization and Computer Grapics*, 4(2):109–116, 1998. 1
18. A. Telea and J.J. van Wijk. Simplified representation of vector fields. In *Proc. IEEE Visualization '99*, pages 35–42, 1999. 2
19. H. Theisel. Designing 2D vector fields of arbitrary topology. *Computer Graphics Forum (Eurographics 2002)*, 21(3):595–604, 2002. 2, 9
20. H. Theisel and T. Weinkauf. Vector field metrics based on distance measures of first order critical points. In *Journal of WSCG, Short Communication*, volume 10, pages 121–128, 2002. 4
21. X. Tricoche, G. Scheuermann, and H. Hagen. A topology simplification method for 2D vector fields. In *Proc. IEEE Visualization 2000*, pages 359–366, 2000. 1
22. X. Tricoche, G. Scheuermann, and H. Hagen. Continuous topology simplification of planar vector fields. In *Proc. Visualization 01*, pages 159 – 166, 2001. 2
23. I. Trotts, D. Kenwright, and R. Haimes. Critical points at infinity: a missing link in vector field topology. In *Proc. NSF/DoE Lake Tahoe Workshop on Hierarchical Approximation and Geometrical Methods for Scientific Visualization*, 2000. 1
24. R. Westermann, C. Johnson, and T. Ertl. Topology-preseving smoothing of vector fields. *IEEE Transactions on Visualization and Computer Graphics*, 7(3):222–229, 2001. 2
25. T. Wischgoll and G. Scheuermann. Detection and visualization of closed streamlines in planar flows. *IEEE Transactions on Visualization and Computer Graphics*, 7(2):165–172, 2001. 1

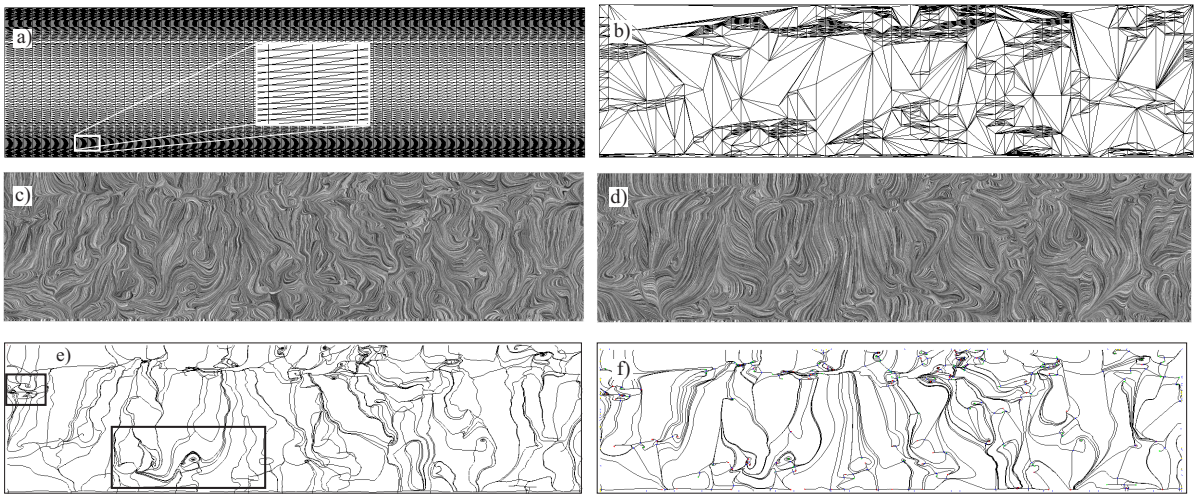

Figure 10: *Test data set 2 (skin friction); a) piecewise triangular domain of the original data set; b) piecewise triangular domain of the compressed data set; c) LIC of original data set; d) LIC of compressed data set; e) topological skeleton of original data set; f) topological skeleton of compressed data set.*

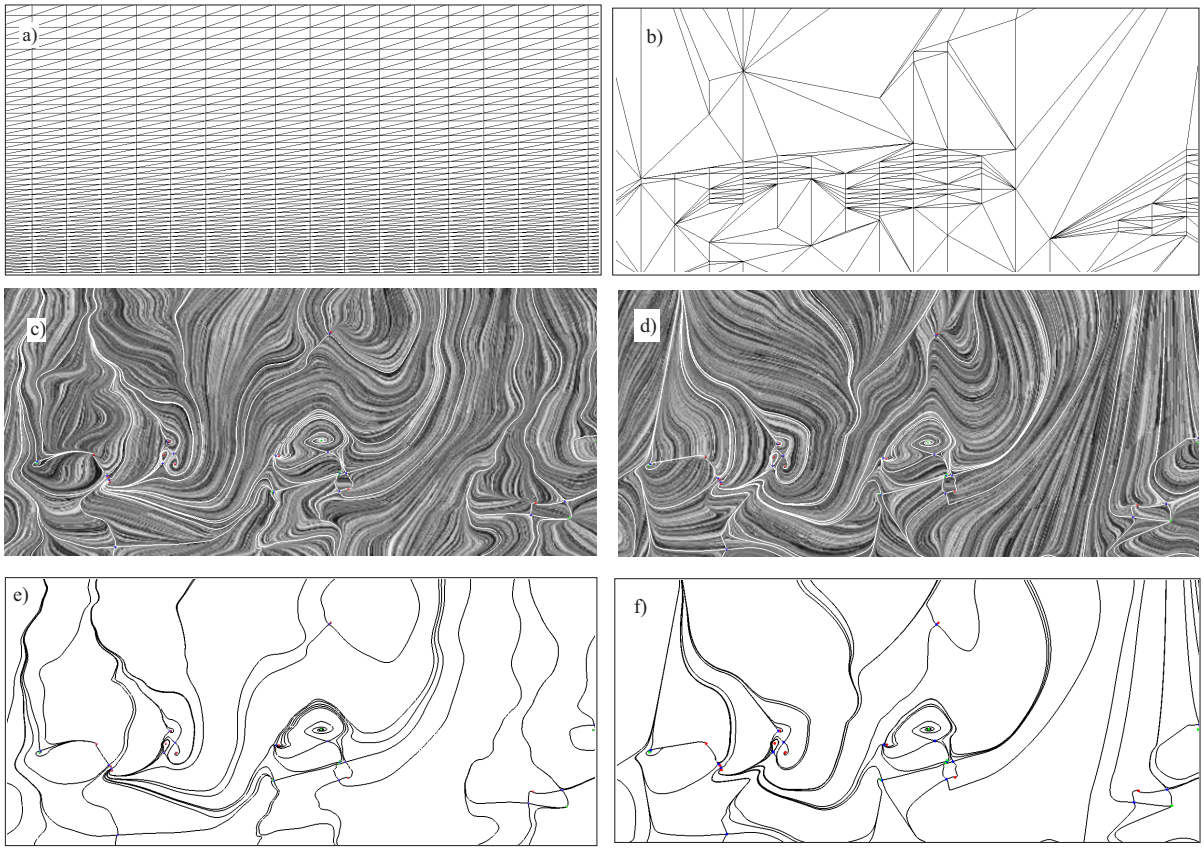

Figure 11: *Magnification of test data set 2; a) piecewise triangular domain of the original data set; b) piecewise triangular domain of the compressed data set; c) LIC of original data set; d) LIC of compressed data set; e) topological skeleton of original data set; f) topological skeleton of compressed data set.*